中國機械工程學刊第四十四卷第一期第 49~58 頁(民國一百一十二年)
Journal of the Chinese Society of Mechanical Engineers, Vol.44, No.1, pp 49~58 (2023)

A Novel Robust Kalman Filter Algorithm With Unknown Noise Statistics for SINS/GPS Integrated Navigation

Xin Lai* and Fu-Xin Yang**

Keywords: Expectation-maximization method, Kalman filter, Uncertain noise, Strapdown inertial navigation system, Global positioning system, Integrated navigation.

ABSTRACT

The estimation of process noise is often inaccurate due to factors such as ambient noise and maneuvering during carrier motion in practical applications. The higher precision and stability of integrated navigation system are pivotal for systems such as vehicles and aircraft. To solve the problem of uncertainty of unknown parameter estimation in the integrated navigation system, a novel robust expectation-maximization based Kalman filter (EM-KF) algorithm is proposed in the paper. The prediction error covariance matrix and measurement noise covariance matrix are estimated adaptively using the online expectation-maximization (EM) method. The remarkable advantages of the EM-KF algorithm in this paper include the following. The online EM is employed to calculate maximum likelihood (ML) estimation of parameters, which converges in each iteration with successive likelihood increments, ensuring local convergence of the iterations; Adaptive estimation of the prediction error covariance matrix and measurement noise covariance matrix can reduce the reliance on prior information and the influence of noise on measurement estimates; The proposed EM-KF has remarkable navigation and robustness in complex environment. Simulations and the field test results illustrate that the proposed EM-KF algorithm has strong robustness and accuracy, and enables high accuracy navigation of moving vehicles for a long time.

Paper Received June, 2022. Revised July, 2022. Accepted August, 2022. Author for Correspondence: Xin Lai.

** Professor, IEEE Senior Member，School of Mechanical and Electrical Engineering, Southwest Petroleum University, Chengdu 610500, China; Oil and Gas Equipment Technology Sharing and Service Platform of Sichuan Province, Chengdu 610500, China; The State Key Laboratory of Oil and Gas Reservoir Geology and Exploitation, Southwest Petroleum University, Chengdu 610500, China.*

***Master Student, School of Mechanical and Electrical Engineering,*

INTRODUCTION

Kalman filter (KF) is an algorithm for optimal estimation of system state and has promoted development in various fields, such as vehicle navigation, unmanned aerial vehicles (UAVs) and aerospace. The navigation accuracy, stability, and safety of these systems are critical. For example, the presence of atmospheric gusts and turbulence can increase the load on the airframe, causing positioning errors and course deviations. KF is a general method to fuse strapdown inertial navigation system (SINS) and Global positioning system (GPS) data. The complete navigation parameters are obtained by gyroscope and accelerometer in SINS continuously, but the accumulative error is its shortcoming. Global Positioning System (GPS) is widely used in navigation, target tracking and other fields since it can acquire its good long-term position accuracy with no cumulative error. However, it will be interfered by obstacles and bad weather (El-Rabbany, 2011; Wang et al., 2021), and GPS signal shielding problems can cause signal loss in environments where GPS signals are unavailable or unreliable. Therefore, the SINS/GPS integrated system provides accurate navigation information for a long time and has better stability (Ning et al., 2019; Li, 2016), which can address the problem of single sensor information loss or unreliability.

The integrated navigation system always assumes the output noise of the sensors as Gaussian distribution (Ren et al., 2021). KF has strong dependence on the prior information of system parameters and noise statistics. Insufficient or wrong information will reduce the accuracy of estimates, and might even lead to divergence. It means that KF cannot achieve high accuracy for navigation in the actual engineering field. Therefore, adaptive KF (AKF) algorithm for uncertain parameter estimation is an urgent problem. Many AKFs for estimating noise statistics are available, such as the Sage-Husa AKF (SHAKF) (Sage et al., 1969; Xu et al., 2019; Wang et al., 2008; Narasimhappa et al., 2012; Liu et al., 2016; Narasimhappa et al., 2020), the Huber-based Kalman filter (HKF) (Wang et al., 2019; Karlgaard and Schaub, 2007; Li et al., 2014-1) and the innovation-based adaptive estimation AKF (IAE-

AKF) (Bian et al., 2006; Fang et al., 2011; Tripathi et al., 2020; Mohamed et al., 1999; Al-Sharman et al., 2018). The SHAKF estimates and modifies system noise statistics in real time using the maximum a posteriori principle, and it can cope with situations with non-zero-mean noise. However, it cannot be guaranteed to converge to the correct noise covariance matrix and may lead to filtering divergence problems, and the error in the filtering result is large when noise covariance matrix is unknown (Wang, 2020). The Huber method performs a correction to the measurement update equations, which is a mixture of minimum ℓ_1- and ℓ_2- norm estimators. In addition, the Huber method finds the optimum of the two estimators to obtain the optimal estimate of the measurement noise (Li et al., 2014-2). In essence, the HKF is utilized to modify the covariance of the measurement noise, but it cannot effectively overcome the high intensity outlier interference (Tseng et al., 2017). According to the ML criterion, the IAE-AKF introduces innovation v_k and its covariance C_{vk} in KF to achieve parameter estimation under unknown and variable noise. However, the accuracy of the IAE method for attitude parameters estimation is related to the quality of SINS, and low-cost SINS will lead to lower precision of estimation (Li et al., 2013). The filter divergence will occur in IAE-AKF where both process noise and measurement noise are not available.

Compared with the previously mentioned filtering algorithm, Expectation maximization (EM) method as an iterative algorithm that uses ML to estimate incomplete parameters with low computational effort, easy implementation and high applicability, such as the adaptive Kalman filter based on EM method (EMAKF) (Huang et al., 2007), which is effective and robust in the integration of GPS/INS system. To enhances the numerical computation, the delta operator model is used in EMAKF for both system state estimation and localization and unknown parameter estimation, replacing the traditional shift operator model, but it will increase the calculation complexity. The EMAKF achieves simultaneous estimation of positioning information and unknown parameters exploiting the offline measurement statistics based on the EM approach. The disadvantage is that it can't implement online parameter estimation. Some AKFs suffers from accuracy degradation in estimating the unknown noise covariance matrix and is not suitable for navigation in uncertain noise environments.

To address the estimation problem of the unknown noise covariance matrix in a complex environment of SINS/GPS, a novel robust EM-KF algorithm is proposed on the basis of EM approach. The contribution points of the EM-KF algorithm are as follows,

(1). The proposed EM-KF algorithm utilize the online EM method to calculate ML parameter estimates with moderate computational complexity and high accuracy. The one-step predicted PDF is approximated as Gaussian, and EM-KF converges in each iteration with successive likelihood increments, ensuring local convergence of iterations.

(2). Adaptive estimation of the covariance matrix of prediction error and measurement noise, rather than the process noise covariance matrix, attenuating the dependence on a priori information, which avoids the need for data windows and can be applied to applications where the noise covariance matrix changes rapidly.

(3). The simulation and field experiment results validate that compare with existing algorithms, the proposed EM-KF has significantly higher navigation precision and robustness in complex environment.

The remainder of this paper is organized as follows. In section II, the attitude, velocity and position error equations in SINS are put forward. The principle and characteristics of KF algorithm are constructed. In section III, the online EM method and robust EM-KF algorithm are proposed. To testify the superiority of the proposed EM-KF algorithm, simulations and field test were conducted in section IV. The conclusion is drawn in section V.

SYSTEM MODEL

The error equations of SINS are an important part of integrated navigation KF state model. In practical application, the inertial sensor inevitably has a measurement error. The position error vector $\boldsymbol{\delta}\mathbf{P}$ is given as $\boldsymbol{\delta}\mathbf{P} = [\delta L,\ \delta\lambda,\ \delta H]$. The position error equations are formulated as (Wang et al., 2021)

$$\delta\dot{L} = \frac{\delta V_N}{R_M + H} - \frac{V_N}{(R_M + H)^2}\delta H \tag{1}$$

$$\delta\dot{\lambda} = \frac{\sec L}{R_N + H}\delta V_E + \frac{V_E \sec L \tan L}{R_N + H}\delta L - \frac{V_E \sec L}{(R_N + H)^2}\delta H \tag{2}$$

$$\delta\dot{H} = \delta V_U \tag{3}$$

where $\{L,\ \lambda,\ H\}$ respectively denote the latitude, longitude and height, and $\{\delta L,\ \delta\lambda,\ \delta H\}$ denote respectively corresponding error of L, λ and H; $\mathbf{V}^{\boldsymbol{n}} = [V_E^n,\ V_N^n,\ V_U^n]$ and $\delta\mathbf{V}^{\boldsymbol{n}} = [\delta V_E^n,\ \delta V_N^n,\ \delta V_U^n\ ]$ are respectively the velocity component and corresponding velocity error component in navigation frame (East-North-Up), and V_E^n , V_N^n and V_U^n are respectively the east, north and up velocity; R_M and R_N denote the radius of principal curvature in the meridian circle and the prime vertical respectively.

The velocity error equation is written as,

$$\delta\dot{\mathbf{V}}^{\boldsymbol{n}} = \left(\boldsymbol{C}_b^n \boldsymbol{f}_{sf}^b\right) \times \boldsymbol{\phi} + \mathbf{V}^{\boldsymbol{n}} \times (2\delta\boldsymbol{\omega}_{ie}^n + \delta\boldsymbol{\omega}_{en}^n) - (2\boldsymbol{\omega}_{ie}^n + \boldsymbol{\omega}_{en}^n) \times \delta\mathbf{V}^n + \boldsymbol{C}_b^n \delta\boldsymbol{f}_{sf}^b \tag{4}$$

where *i*, *e*, *n*, and *b* are respectively the inertial frame, the Earth frame, the navigation frame and the body frame; $\boldsymbol{\omega}_{ie}^{n}$ is the Earth rotation angular rate relative to the inertial frame, and $\boldsymbol{\omega}_{en}^{n}$ denotes the navigation system rotation angular rate relative to the Earth frame, while $\delta\boldsymbol{\omega}_{ie}^{n}$ and $\delta\boldsymbol{\omega}_{en}^{n}$ are corresponding calculation errors respectively; $\delta \boldsymbol{f}_{sf}^{b}$ denotes the accelerometer measurement error along the body frame, and $\boldsymbol{C}_{b}^{n}$ is the attitude transformation matrix from the body frame to the navigation frame. . The symbol $\times$ represents cross product of two vectors.

The attitude error equation is written as,

$$\dot{\boldsymbol{\phi}} = \boldsymbol{\phi} \times \boldsymbol{\omega}_{in}^{n} + \delta\boldsymbol{\omega}_{in}^{n} - \delta\boldsymbol{\omega}_{ib}^{n} \tag{5}$$

where $\boldsymbol{\phi} = [\phi_E,\ \phi_N,\ \phi_U]^T$ denotes the misalignment angle of ideal navigation frame with respect to the calculated navigation frame, and ϕ_E, ϕ_N and ϕ_U are errors of pitch, roll and heading respectively, $\boldsymbol{\omega}_{in}$ and $\delta\boldsymbol{\omega}_{in}$ are respectively the angular rate of the navigation framework relative to the inertial frame and corresponding calculated error, and $\delta\boldsymbol{\omega}_{ib}$ denotes the gyroscope measurement error.

Therefore, the error state vector of the KF is written as: $\delta\mathbf{X} = [\boldsymbol{\phi}^T,\ (\delta\mathbf{V})^T,\ (\delta\mathbf{P})^T,\ (\delta\mathbf{b}_w)^T, (\delta\mathbf{b}_f)^T]^T$, where $\delta\mathbf{b}_w$ and $\delta\mathbf{b}_f$ are respectively error in gyroscope bias and accelerometer bias, which are modeled as random walk processes. Accordingly, the linearized system error model can be written as follows (Li et al., 2020),

$$\delta\dot{\mathbf{X}}_k = \mathbf{F}\delta\mathbf{X}_{k-1} + \mathbf{w}_{k-1} \tag{6}$$

where $\mathbf{F}$ denotes the state transition matrix, $\mathbf{w}_k$ denotes the process noise whose expected value is $E[\mathbf{w}_k]$=0 and satisfies $E[\mathbf{w}_k\mathbf{w}_k^T]$= $\mathbf{Q}_k$, and $E[\cdot]$ stands for expected value operation.

The bias between the position change estimated by SINS and GPS forms the observation vector in the observation model, so the observation vector is defined as is defined as follows,

$$\mathbf{Z}_k = \begin{bmatrix} L_{SINS} - L_{GPS} \\ \lambda_{SINS} - \lambda_{GPS} \\ H_{SINS} - H_{GPS} \end{bmatrix} = \mathbf{H}\delta\mathbf{X}_k + \mathbf{v}_{k-1} \tag{7}$$

where $\mathbf{Z}_k$ is the measurement vector, the subscript SINS and GPS represent the observations from SINS and GPS respectively, $\mathbf{H}$ denotes the measurement matrix, $\mathbf{v}_k$ is the measurement noise whose expected value is $E[\mathbf{v}_k]$=0 and satisfies $E[\mathbf{v}_k\mathbf{v}_k^T]$= $\mathbf{R}_k$. In addition, $\mathbf{w}_k$ and $\mathbf{v}_k$ are independent, that is, $E[\mathbf{w}_k\mathbf{v}_k^T]$=0.

The KF is composed of predicted and updated stage. In the predicted stage, the state vector is predicted through the state vector at the previous time, it can be formulated as,

$$\hat{\mathbf{X}}_{k|k-1}^{-} = \mathbf{F}\hat{\mathbf{X}}_{k-1|k-1} \tag{10}$$

$$\mathbf{P}_{k|k-1} = \mathbf{F}\mathbf{P}_{k-1|k-1}\mathbf{F}^{\mathrm{T}} + \mathbf{Q}_{k-1} \tag{11}$$

where $\hat{\mathbf{X}}_{k|k-1}^{-}$ and $\mathbf{P}_{k|k-1}$ denote the predicted state vector and corresponding predicted error covariance matrix respectively.

In the updated stage, the measurement vector is employed to update the current state vector, which is defined as

$$\mathbf{K}_k = \mathbf{P}_{k|k-1}\mathbf{H}_k^T\left(\mathbf{H}_k\mathbf{P}_{k|k-1}\mathbf{H}_k^{\mathrm{T}} + \mathbf{R}_k\right)^{-1} \tag{12}$$

$$\hat{\mathbf{X}}_{k|k} = \hat{\mathbf{X}}_{k|k-1}^{-} + \mathbf{K}_k\left(\mathbf{Z}_{\mathrm{k}} - \mathbf{H}_k\hat{\mathbf{X}}_{k|k-1}^{-}\right) \tag{13}$$

$$\mathbf{P}_{k|k} = (\mathbf{I} - \mathbf{K}_k\mathbf{H}_k)\mathbf{P}_{k|k-1} \tag{14}$$

where $\hat{\mathbf{X}}_{k|k}$ and $\mathbf{P}_{k|k}$ are the state estimate vector and corresponding estimation error covariance matrix respectively; $\mathbf{Z}_k$ denotes the measurement vector, $\mathbf{K}_k$ denotes the Kalman gain and $(\cdot)^{-1}$ means the inversion operation of a matrix, and I denotes the ，.

Kalman filtering algorithm is used to filter and fuse each sensor output of integrated navigation according to the optimal estimation criterion, and it can obtain the precise position and corresponding parameter information when noises are modeled as Gaussian white processes. However, KF is a filtering algorithm with minimum mean square error (MMSE) in linear state space models that models the process and measurement noise are modeled as a Gaussian process. When Kalman filtering is applied in integrated navigation, optimality may be destroyed due to unreliable sensors, non-Gaussian noises making the state estimates less accurate and even divergent (Feng et al., 2021; Li et al., 2014; Lai et al., 2021; Qian et al., 2010). To solve the above problem, a robust EM-KF algorithm is proposed using EM method to estimate covariance matrix of the predicted and the measurement noise adaptively.

A NOVEL ROBUST EM-KF ALGORITHM

The EM method is an iterative algorithm to generate the ML estimate or maximum a posteriori estimates of parameters in a probability model. The EM method including the E-step and the M-step. It has a prominent advantage of guaranteeing that successive iterations always yield a likelihood-increasing estimated parameter. In this paper, the aim is to online estimate the uncertain Pk and $\mathbf{R}_k$ and through the measured value $\mathbf{Z}_k$ (Huang er al., 2018). The collection of measured values is set as the incomplete data $\mathbf{Z}$ and $\mathbf{Z} \triangleq \{\mathbf{Z}_1,\ \mathbf{Z}_2, \dots, \mathbf{Z}_k\}$, which denotes the measurement from time 1 to k.

Meanwhile, the collection of state estimate values and measurement values is set as the complete data $\mathbf{C}$ and $\mathbf{C} \triangleq \{\mathbf{X}_1, \dots,\ \mathbf{X}_k,\ \mathbf{Z}_1,\ \mathbf{Z}_2, \dots, \mathbf{Z}_k\}$.

The EM algorithm iterates between two steps. We define $\boldsymbol{\theta}_k \triangleq \{\mathbf{P}_{k|k-1},\ \mathbf{R}_k\}$. The traditional definition of the log-likelihood function is as follows,

$$L\ (\boldsymbol{\theta}_k|\mathbf{Z}) \triangleq \log\ p\ (\mathbf{Z}|\boldsymbol{\theta}_k) \tag{15}$$

where log $(\cdot)$ is the logarithm operation and $p\ (\mathbf{Z}|\boldsymbol{\theta}_k)$ denotes a probability density function (PDF) that depends on $\boldsymbol{\theta}_k$. Employing the relationship of the conditional PDF and the joint PDF, the above equation will be modified to

$$\log\ p\ (\mathbf{Z}|\boldsymbol{\theta}_k) = \log\ p\ (\mathbf{X}_k, \mathbf{Z}|\boldsymbol{\theta}_k) - \log\ p\ (\mathbf{X}_k|\mathbf{Z}, \boldsymbol{\theta}_k) \quad (16)$$

In E-step, integrate both sides of Eq. (16) with respect to $p\ (\mathbf{X}_k|\mathbf{Z}, \boldsymbol{\theta}_k^{(i)})$, which is also the expectation with respect to $p\left(\mathbf{X}_k \middle| \mathbf{Z}, \boldsymbol{\theta}_k^{(i)}\right)$, and the result is,

$$L(\boldsymbol{\theta}_k|\mathbf{Z}) = \int \log p\ (\mathbf{X}_k, \mathbf{Z}|\boldsymbol{\theta}_k) p\ (\mathbf{X}_k \middle| \mathbf{Z}, \boldsymbol{\theta}_k^{(i)}) d\mathbf{X}_k - \int \log p\ (\mathbf{X}_k|\mathbf{Z}, \boldsymbol{\theta}_k) p\ (\mathbf{X}_k \middle| \mathbf{Z}, \boldsymbol{\theta}_k^{(i)}) d\mathbf{X}_k \quad (17)$$

where $\boldsymbol{\theta}_k^{(i)}$ denotes an approximation of $\boldsymbol{\theta}_k$ at the i-th step. We define $Q\left(\boldsymbol{\theta}_k, \boldsymbol{\theta}_k^{(i)}\right) \triangleq \int \log p\ (\mathbf{X}_k, \mathbf{Z}|\boldsymbol{\theta}_k) p\ (\mathbf{X}_k \middle| \mathbf{Z}, \boldsymbol{\theta}_k^{(i)}) d\mathbf{X}_k$ and $H\left(\boldsymbol{\theta}_k, \boldsymbol{\theta}_k^{(i)}\right) \triangleq \int \log p\ (\mathbf{X}_k|\mathbf{Z}, \boldsymbol{\theta}_k) p\ (\mathbf{X}_k \middle| \mathbf{Z}, \boldsymbol{\theta}_k^{(i)}) d\mathbf{X}_k$. Substituting the $\boldsymbol{\theta}_k$ into $\boldsymbol{\theta}_k^{(i)}$ in the $H\left(\boldsymbol{\theta}_k, \boldsymbol{\theta}_k^{(i)}\right)$, the following equations can be obtained,

$$H\left(\boldsymbol{\theta}_k^{(i)}, \boldsymbol{\theta}_k^{(i)}\right) = \int \log p\ \left(\mathbf{X}_k|\mathbf{Z}, \boldsymbol{\theta}_k^{(i)}\right) p\ (\mathbf{X}_k|\mathbf{Z}, \boldsymbol{\theta}_k^{(i)}) d\mathbf{X}_k \quad (18)$$

Subtracting $H\left(\boldsymbol{\theta}_k, \boldsymbol{\theta}_k^{(i)}\right)$ from $H\left(\boldsymbol{\theta}_k^{(i)}, \boldsymbol{\theta}_k^{(i)}\right)$, and we can obtain,

$$H\left(\boldsymbol{\theta}_k, \boldsymbol{\theta}_k^{(i)}\right) - H\left(\boldsymbol{\theta}_k^{(i)}, \boldsymbol{\theta}_k^{(i)}\right) = \int p\ (\mathbf{X}_k \middle| \mathbf{Z}, \boldsymbol{\theta}_k^{(i)}) \log \frac{(\mathbf{X}_k|\mathbf{Z}, \boldsymbol{\theta}_k)}{\left(\mathbf{X}_k|\mathbf{Z}, \boldsymbol{\theta}_k^{(i)}\right)} d\mathbf{X}_k = -\mathrm{KL}\left(p\left(\mathbf{X}_k|\mathbf{Z}, \boldsymbol{\theta}_k^{(i)}\right) \parallel p(\mathbf{X}_k|\mathbf{Z}, \boldsymbol{\theta}_k)\right) \quad (19)$$

The following relationship can be obtained according to Eq. (17) and Eq. (19),

$$L(\boldsymbol{\theta}_k|\mathbf{Z}) - L\left(\boldsymbol{\theta}_k^{(i)}|\mathbf{Z}\right) = Q\left(\boldsymbol{\theta}_k, \boldsymbol{\theta}_k^{(i)}\right) - Q\left(\boldsymbol{\theta}_k^{(i)}, \boldsymbol{\theta}_k^{(i)}\right) + \mathrm{KL}\left(p\left(\mathbf{X}_k|\mathbf{Z}, \boldsymbol{\theta}_k^{(i)}\right) \parallel p(\mathbf{X}_k|\mathbf{Z}, \boldsymbol{\theta}_k)\right) \quad (20)$$

where KL denotes the Kullback–Leibler divergence, and it satisfies the equation $\mathrm{KL}(p(x) \parallel q(x)) \triangleq \int p(x) log \frac{p(x)}{q(x)} dx$ (Li et al., 2016). We know that $\mathrm{KL}(p(x) \parallel q(x)) \geq 0$, where the equation denotes Evidence Lower Bound (ELBO). Considering that KL is non-negative, we can obtain the following relationship,

$$L\ (\boldsymbol{\theta}_k|\mathbf{Z}) - L\left(\boldsymbol{\theta}_k^{(i)}|\mathbf{Z}\right) \geq Q\left(\boldsymbol{\theta}_k, \boldsymbol{\theta}_k^{(i)}\right) - Q\left(\boldsymbol{\theta}_k^{(i)}, \boldsymbol{\theta}_k^{(i)}\right) \quad (21)$$

If we employ $\boldsymbol{\theta}_k^{(i+1)}$ to substitute $\boldsymbol{\theta}_k$ in Eq. (21), so we can obtain $Q\left(\boldsymbol{\theta}_k^{(i+1)}, \boldsymbol{\theta}_k^{(i)}\right) \geq Q\left(\boldsymbol{\theta}_k^{(i)}, \boldsymbol{\theta}_k^{(i)}\right)$, thus, $L\left(\boldsymbol{\theta}_k^{(i+1)}|\mathbf{Z}\right) \geq L\left(\boldsymbol{\theta}_k^{(i)}|\mathbf{Z}\right)$, which means that the parameter $\boldsymbol{\theta}_k$ will not decrease during the iteration. The maximum value of $Q\left(\boldsymbol{\theta}_k, \boldsymbol{\theta}_k^{(i)}\right)$ can be regarded as the optimal estimation of $L_{\boldsymbol{\theta}_k}(\mathbf{Z}_{1:k})$, when $i \to +\infty$ using Eq. (21). Therefore, we can obtain the ML estimate of $\boldsymbol{\theta}_k$ by EM method, while ensuring convergence of the iterations.

In this paper, the measurement $\mathbf{Z}$ is related to $\mathbf{X}_k$, so the log-likelihood function in Eq. (15) will be modified as,

$$L\ (\boldsymbol{\theta}_k|\mathbf{X}_k, \mathbf{Z}) \triangleq \log\ p\ (\mathbf{X}_k, \mathbf{Z}|\boldsymbol{\theta}_k) \quad (22)$$

And the EM algorithm comprise $E_{\mathbf{X}_k|\mathbf{Z}, \boldsymbol{\theta}_k^{(i)}}[\log p\ (\mathbf{X}_k, \ \mathbf{Z}|\boldsymbol{\theta}_k)]$ in E-step and $\arg max_{\boldsymbol{\theta}_k} Q(\boldsymbol{\theta}_k, \boldsymbol{\theta}_k^{(i)})$ in M-step. Finally, the estimated value of the parameter $\boldsymbol{\theta}_k$ will be obtained through iteration. Thus, the E-step can be acquired by calculating its estimate as follows (Schön et al., 2011; Huang et al., 2017),

$$L\ (\boldsymbol{\theta}_k|\mathbf{X}_k, \mathbf{Z}) \approx Q\left(\boldsymbol{\theta}_k, \boldsymbol{\theta}_k^{(i)}\right) \triangleq E_{\mathbf{X}_k|\mathbf{Z}, \boldsymbol{\theta}_k^{(i)}}[\log p\ (\mathbf{X}_k, \ \mathbf{Z}|\boldsymbol{\theta}_k)] = \int \log p\ (\mathbf{X}_k, \mathbf{Z}|\boldsymbol{\theta}_k) p\ (\mathbf{X}_k \middle| \mathbf{Z}, \boldsymbol{\theta}_k^{(i)}) d\mathbf{X}_k \quad (23)$$

where $E_{\mathbf{X}_k|\mathbf{Z}, \boldsymbol{\theta}_k^{(i)}}[\cdot]$ is the exception with regard to $\mathbf{X}_k$, $\boldsymbol{\theta}_k^{(i)}$ denotes an approximation of $\boldsymbol{\theta}_k$ at the i-th step.

According to Eq. (23), we need to calculate $\log p\ (\mathbf{X}_k, \mathbf{Z}|\boldsymbol{\theta}_k)$ and $p\ (\mathbf{X}_k \middle| \mathbf{Z}, \boldsymbol{\theta}_k^{(i)})$ in advance to prepare for calculation of $Q\left(\boldsymbol{\theta}_k, \boldsymbol{\theta}_k^{(i)}\right)$. In the light of Bayesian theorem, the joint log-likelihood function $p_{\boldsymbol{\theta}_k}(\mathbf{X}_k, \ \mathbf{Z}_{1:k})$ will be expressed,

$$\begin{aligned}
&\log p\ (\mathbf{X}_k, \mathbf{Z}|\boldsymbol{\theta}_k) \\
&= \log\ p\ (\mathbf{Z}_k|\mathbf{X}_k, \ \mathbf{Z}_{1:k-1}, \boldsymbol{\theta}_k) p(\mathbf{X}_k|\mathbf{Z}_{1:k-1}, \boldsymbol{\theta}_k) p(\mathbf{Z}_{1:k-1}) \\
&= log\ p(\mathbf{Z}_k|\mathbf{X}_k, \boldsymbol{\theta}_k) p(\mathbf{X}_k|\mathbf{Z}_{1:k}, \boldsymbol{\theta}_k) p(\mathbf{Z}_{1:k-1}) \\
&= -0.5 \log|\mathbf{R}_k| - 0.5 \log\left|\mathbf{P}_{k|k-1}\right| + C_{\boldsymbol{\theta}_k} \\
&\quad -0.5(\mathbf{X}_k - \hat{\mathbf{X}}_{k|k-1})^T \mathbf{P}_{k|k-1}^{-1} \left(\mathbf{X}_k - \hat{\mathbf{X}}_{k|k-1}\right)
\end{aligned} \quad (24)$$

where $|\cdot|$ denotes the determinant operation of a matrix and $C_{\boldsymbol{\theta}_k}$ is the constant associated with $\boldsymbol{\theta}_k$. $p(\mathbf{Z}_{1:k-1})$ don't rely on parameter $\boldsymbol{\theta}_k$ because $\mathbf{Z}_{1:k-1}$ is independent from $\mathbf{P}_{k|k-1}$ and $\mathbf{R}_k$. $p\ (\mathbf{X}_k \middle| \mathbf{Z}_{1:k}, \boldsymbol{\theta}_k^{(i)})$ denotes the posterior PDF, which is also the one-step prediction PDF and it is defined as follows,

$$p\ (\mathbf{X}_k \middle| \mathbf{Z}_{1:k}, \boldsymbol{\theta}_k^{(i)}) \triangleq N\left(\mathbf{X}_k; \hat{\mathbf{X}}_{k|k}^{(i+1)}, \mathbf{P}_{k|k}^{(i+1)}\right) \quad (25)$$

where $N(\cdot)$ represents the Multivariate Gaussian Distribution, and $\hat{\mathbf{X}}_{k|k}^{(i+1)}$ and $\mathbf{P}_{k|k}^{(i+1)}$ are obtained according to Eq. (12) - Eq. (14), the iteration progress of measurement update are as follows,

$$\mathbf{K}_k^{(i+1)} = \mathbf{P}_{k|k-1}^{(i)} (\mathbf{H}_k^{(i)})^T [\mathbf{H}_k^{(i)} \mathbf{P}_{k|k-1}^{(i)} (\mathbf{H}_k^{(i)})^T + \mathbf{R}_k^{(i)}]^{-1} \quad (26)$$

$$\hat{\mathbf{X}}_{k|k}^{(i+1)} = \hat{\mathbf{X}}_{k|k-1}^{-} + \mathbf{K}_k^{(i+1)} \left(\mathbf{Z}_k - \mathbf{H}_k^{(i)} \hat{\mathbf{X}}_{k|k-1}^{-}\right) \quad (27)$$

$$\mathbf{P}_{k|k}^{(i+1)} = \mathbf{P}_{k|k-1}^{(i)} - \mathbf{K}_k^{(i+1)} \mathbf{H}_k^{(i)} \mathbf{P}_{k|k-1}^{(i)} \quad (28)$$

Substituting Eq. (24) and Eq. (25) into Eq. (23), we can obtain a new form of $Q(\boldsymbol{\theta}_k,\ \boldsymbol{\theta}_k^{(i)})$ by a series of mathematical calculations,

$$\begin{aligned} &Q(\boldsymbol{\theta}_k,\ \boldsymbol{\theta}_k^{(i)}) \\ &= -0.5\log|\mathbf{R}_k| - 0.5tr(\mathbf{A}_k\mathbf{R}_k^{-1}) - 0.5\log|\mathbf{P}_{k|k-1}| \\ &\quad -0.5tr(\mathbf{B}_k\mathbf{P}_{k|k-1}^{-1}) + C_{\boldsymbol{\theta}_k} \end{aligned} \tag{29}$$

where tr (·) denotes the trace of a matrix, $\mathbf{A}_k$ and $\mathbf{B}_k$ are expressed respectively as follows,

$$\begin{aligned} \mathbf{A}_k = &(\mathbf{Z}_k - \mathbf{H}_k^{(i+1)}\widehat{\mathbf{X}}_{k|k-1}^{-})(\mathbf{Z}_k - \mathbf{H}_k^{(i+1)}\widehat{\mathbf{X}}_{k|k-1}^{-})^T \\ &+\mathbf{H}_k^{(i+1)}\mathbf{P}_{k|k}^{(i+1)}(\mathbf{H}_k^{(i+1)})^T \end{aligned} \tag{30}$$

$$\begin{aligned} \mathbf{B}_k = &\mathbf{P}_{k|k}^{(i+1)} \\ &+(\widehat{\mathbf{X}}_{k|k}^{(i+1)} - \widehat{\mathbf{X}}_{k|k-1}^{-})(\widehat{\mathbf{X}}_{k|k}^{(i+1)} - \widehat{\mathbf{X}}_{k|k-1}^{-})^T \end{aligned} \tag{31}$$

The ML estimate is used to find the parameter $\boldsymbol{\theta}_k$, which will be obtained in the M-step and the equation is as follows,

$$\boldsymbol{\theta}_k^{(i+1)} \approx \arg max_{\boldsymbol{\theta}_k} Q(\boldsymbol{\theta}_k,\ \boldsymbol{\theta}_k^{(i)}) \tag{32}$$

where $\widehat{\boldsymbol{\theta}}_k$ is the ML estimate of $\boldsymbol{\theta}_k$ and $p(\mathbf{X}_k, \mathbf{Z}|\boldsymbol{\theta}_k\ \cdot)$ is the PDF of the complete data that depends on $\boldsymbol{\theta}_k$, $\boldsymbol{\theta}_k^{(i+1)}$ represents the approximation of $\widehat{\boldsymbol{\theta}}_k$ of the i+1th iteration.

In this step, the approximation of $\boldsymbol{\theta}_k$ is obtained by calculating the maximization of $Q(\boldsymbol{\theta}_k,\ \boldsymbol{\theta}_k^{(i)})$ through Eq. (29). According to the relationship between the derivative and the extremum, the $\boldsymbol{\theta}_k^{(i+1)}$ should satisfy the following formula,

$$\left.\frac{\partial Q(\boldsymbol{\theta}_k,\ \boldsymbol{\theta}_k^{(i)})}{\partial \boldsymbol{\theta}_k}\right|_{\boldsymbol{\theta}_k = \boldsymbol{\theta}_k^{(i+1)}} = 0 \tag{33}$$

$\boldsymbol{\theta}_k \triangleq \{\mathbf{P}_{k|k-1}, \mathbf{R}_k\}$ is defined, so Eq. (33) can be transformed into as follows,

$$\left.\frac{\partial Q(\boldsymbol{\theta}_k,\ \boldsymbol{\theta}_k^{(i)})}{\partial \mathbf{P}_{k|k-1}}\right|_{\mathbf{P}_{k|k-1}=\mathbf{P}_{k|k-1}^{(i+1)},\ \mathbf{R}_k=\mathbf{R}_k^{(i+1)}} = 0 \tag{34}$$

$$\left.\frac{\partial Q(\boldsymbol{\theta}_k,\ \boldsymbol{\theta}_k^{(i)})}{\partial \mathbf{R}_{k|k-1}}\right|_{\mathbf{P}_{k|k-1}=\mathbf{P}_{k|k-1}^{(i+1)},\ \mathbf{R}_k=\mathbf{R}_k^{(i+1)}} = 0 \tag{35}$$

Employing Eq. (29), the partial derivatives of Eq. (34) and Eq. (35) can be calculated, and the results are as follows,

$$\frac{\partial Q(\boldsymbol{\theta}_k, \boldsymbol{\theta}_k^{(i)})}{\partial \mathbf{P}_{k|k-1}} = -0.5\mathbf{P}_{k|k-1}^{-1} + 0.5\mathbf{P}_{k|k-1}^{-1}\mathbf{B}_k\mathbf{P}_{k|k-1}^{-1} = 0 \tag{36}$$

$$\frac{\partial Q(\boldsymbol{\theta}_k,\ \boldsymbol{\theta}_k^{(i)})}{\partial \mathbf{R}_{k|k-1}} = -0.5\mathbf{R}_k^{-1} + 0.5\mathbf{R}_k^{-1}\mathbf{A}_k\mathbf{R}_k^{-1} = 0 \tag{37}$$

After computing Eq. (36) and Eq. (37), we can solve to get $\mathbf{P}_{k|k-1}^{(i+1)}$ and $\mathbf{R}_k^{(i+1)}$,

$$\mathbf{P}_{k|k-1}^{(i+1)} = \mathbf{B}_k \tag{38}$$

$$\mathbf{R}_k^{(i+1)} = \mathbf{A}_k \tag{39}$$

Thus, employing Eq. (30), Eq. (31) and Eq. (38), Eq. (39) to carry out the iterative cycle of Kalman filter. After iteration *S*, the state estimate $\widehat{\mathbf{X}}_{k|k}$ and corresponding estimation error covariance matrix $\mathbf{P}_{k|k}$, the predicted error covariance matrix $\widehat{\mathbf{P}}_{k|k-1}$, and the estimate of measurement noise covariance matrix $\widehat{\mathbf{R}}_k$ are obtained as follows,

$$\widehat{\mathbf{X}}_{k|k} = \widehat{\mathbf{X}}_{k|k}^{(S)}, \qquad \mathbf{P}_{k|k} = \mathbf{P}_{k|k}^{(S)} \tag{40}$$

$$\widehat{\mathbf{P}}_{k|k-1} = \mathbf{P}_{k|k-1}^{(S)}, \qquad \widehat{\mathbf{R}}_k = \mathbf{R}_k^{(S)} \tag{41}$$

SIMULATIONS AND FIELD TEST

Simulations

In this case, the designed trajectory is tracked using the SINS and the proposed algorithm, respectively. The designed trajectory includes uniform, accelerating and decelerating motion and spiral upward motion. The total time is 595 s and the sampling interval is T=0.01. The bias of gyro constant and the accelerometer constant are respectively set as 0.01 °/h and 100 μg. $\mathrm{H_K} = [\ 0_{3\times6}\ \mathbf{I}_3\ 0_{3\times6}]$, and $\mathbf{I}_3$ is the 3-D identity matrix.

Three-dimensional position of the true trajectory, GPS, SINS and the proposed EM-KF is shown in Figure 1. The SINS only uses IMU data for updates, and GPS's data are simulation data derived from the position parameters of the true trajectory plus the white noise. The proposed EM-KF is employed to process the bias between SINS and GPS in the integrated SINS/GPS navigation system. The starting point and the ending point are respectively represented by the black symbol '☆' and '*'.

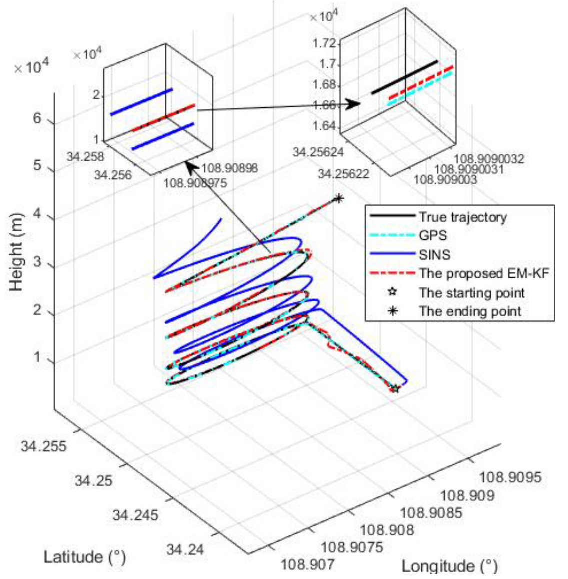

Fig. 1. Three-dimensional position comparison of true trajectory, GPS, SINS and the proposed EM-KF.

Fig. 1 shows that the trajectory of the proposed EM-KF deviates from the true trajectory in the beginning stage, but gradually consists with it roughly after algorithm correction. The proposed algorithm obviously has more accurate trajectory than SINS, and it tend to the true trajectory better, while the trajectory of SINS gradually deviates from the true trajectory. It is due to the fact that SINS's error increases and accumulates over time. The results illustrates that the proposed EM-KF has significantly better tracking navigation capability than SINS.

The parameter of the true trajectory, SINS and the proposed EM-KF are presented in Figure 2 and Figure 3 respectively. The parameter of the true trajectory, GPS, SINS and the proposed EM-KF is shown in Figure 4. Fig. 2 illustrates that the attitude of the proposed EM-KF is roughly consistent with that of SINS. We can see from Fig. 3 and Fig. 4 that the tracking accuracy of velocity and position is obviously superior to that of SINS, for only the velocity and position parameter are filtered by the proposed algorithm. Thus, it is concluded that the proposed EM-KF outperforms the SINS in velocity and position estimation accuracy.

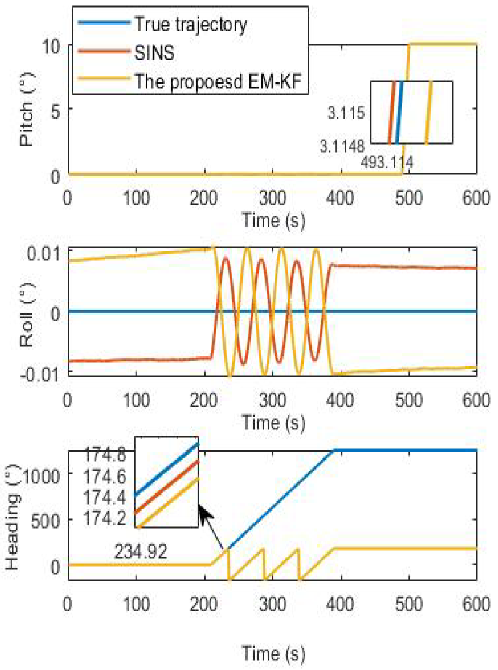

Fig. 2. Attitude of true trajectory, SINS and the proposed EM-KF.

Car-mounted field test

To verify the advantage of the proposed EK-KF algorithm based on loosely-coupled SINS/GPS integration in practice, the experiment was conducted on the moving car. The car moved slowly over the campus of Southwest Petroleum University in a good weather. Therefore, it can receive GPS signals without obstruction and make GPS work normally to obtained valid position and navigation information. In the field test, the total driving distance is 1.12km. We employed the proposed algorithm for navigation and the relevant parameters of moving vehicle are recorded. The data of parameters of SINS is also obtained and stored at the same time.

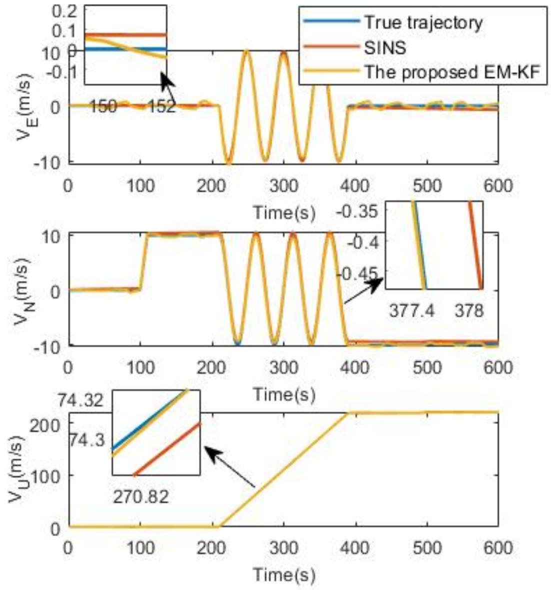

Fig. 3. Velocity of true trajectory, SINS and the proposed EM-KF.

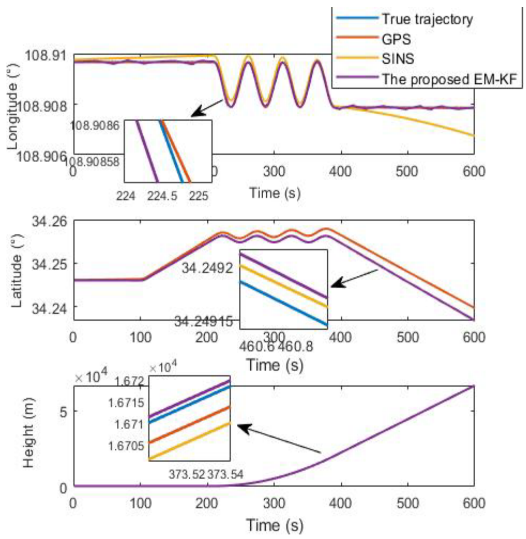

Fig. 4. Position of true trajectory, GPS, SINS and the proposed EM-KF.

The parameters of GPS, SINS and the proposed EM-KF including velocity and position are respectively shown in Fig. 5 and Fig. 6. Fig. 5 shows that the velocity of the proposed algorithm in the proposed EM-KF is almost same as that of SINS. Since the velocity parameters do not participate in the filtering process of the proposed EM-KF in the SINS/GPS integrated system, it has large error than that of the position parameters. In Fig. 6, the velocity and position parameters of the proposed EM-KF are more accurate and robust than that of SINS, and roughly consistent with GPS, which has stronger robustness for navigation in reality. Table 1 shows the Standard Deviation (STD) and Root Mean Squared

Error (RMSE) of errors from different methods. The STD of the proposed method is smaller than that of SINS, which represents that the error fluctuation of the proposed EM-KF is less. Similarly, the RMSE of the proposed EM-KF is significantly smaller than that of the SINS.

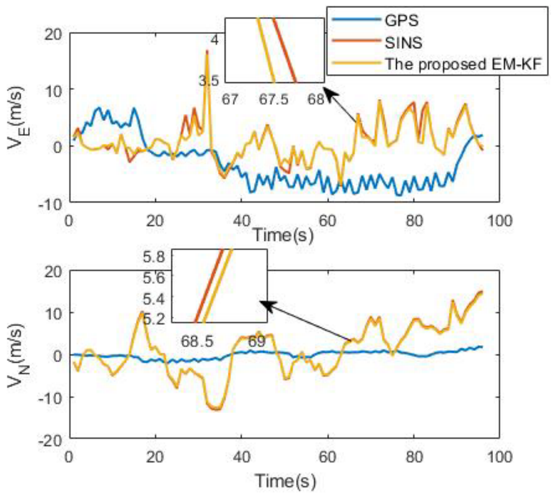

Fig. 5. The velocity from GPS, SINS and the proposed EM-KF.

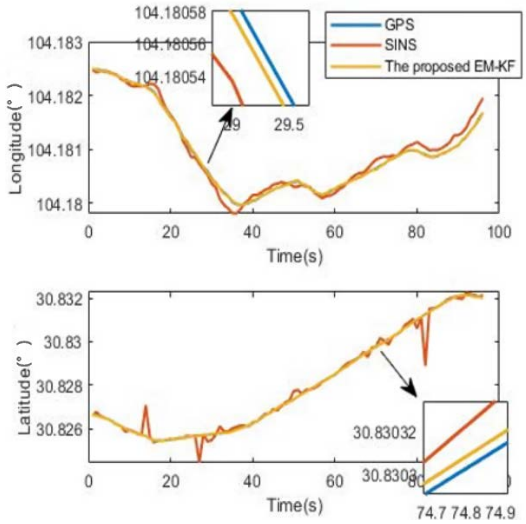

Fig. 6. The position from GPS, SINS and the proposed EM-KF.

Table 1. Specific data for the tank vehicle.

State	Algorithms	STD	RMSE
Error of V_E (m/s)	SINS Proposed method	3.907 3.673	6.858 6.499
Error of V_N (m/s)	SINS Proposed method	3.385 3.244	5.741 5.503
Error of longitude (º)	SINS Proposed method	1.15E-06 9.61E-08	1.932e-06 1.587e-07
Error of latitude (º)	SINS Proposed method	5.32E-06 8.99E-08	5.758e-06 1.587e-07
Error of height (m)	SINS Proposed method	2202.337 5.344	6080.136 6.116

The trajectory of the moving vehicle was recorded in real time by the navigation application on the mobile phone and the results is recorded in Figure 7. In Fig. 7, the car traveled around the campus, including multiple straight and turn movements, and the true trajectory is provided by the GPS. The comparison of GPS, SINS and the proposed EM-KF implemented on the SINS/GPS integrated system is demonstrated in Figure 8.

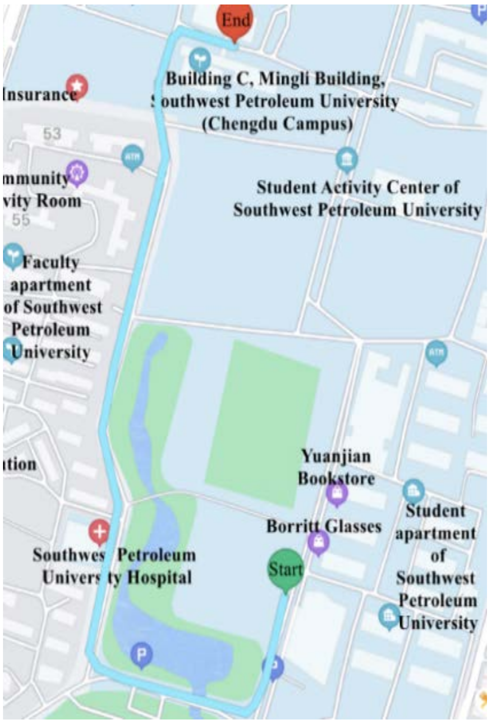

Fig. 7. The experimental trajectory was recorded by navigation application on mobile phone.

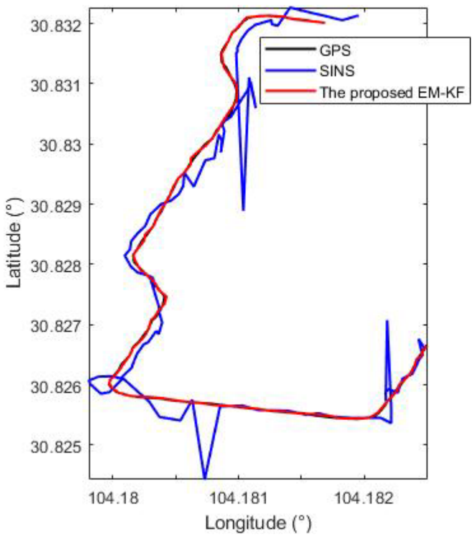

Fig. 8. Real-time trajectory of GPS, SINS and the proposed EM-KF.

As shown in Fig. 8, the trajectory of SINS undergoes a sharp and abrupt change, especially in the vehicle turn. That's due to the fact that when the vehicle turns, the attitude and position change sharply compared to smooth driving, together with the integration accumulated error of SINS, resulting in a large position error of SINS. On the contrast, the trajectory of the proposed algorithm is clearly smooth and accurate, and its trajectory is almost consistent with the true trajectory. After filtering by our proposed algorithm, the tracking accuracy is enhanced and the navigation capability is improved. The car-mounted experiment indicates that the proposed EM-KF algorithm on the SINS/GPS has higher tracking accuracy and stronger robustness, which better decreases the accumulated error of SINS and the effect of the sensor measurement noise.

CONCLUSIONS

In this paper, the new EM-KF algorithm is proposed to adaptively estimate the predicted error covariance matrix and measurement noise covariance matrix. The proposed algorithm utilizes the online EM method to calculate ML parameter estimates. It weakens the dependence on prior information, and is suitable for inaccurate noise covariance matrices and unknown parameter estimation. Simulation and Experiment results demonstrate that the proposed EM-KF algorithm has higher filtering accuracy and robustness than existing algorithms, and can be applied to optimization the performance and reliability of the navigation system. The idea of this paper can be extended to multi-sensor fusion algorithms, such as SINS/GPS/LiDAR (light detection and ranging) system in the future work.

REFERENCES

Al-Sharman, M.K., Jaradat, M.A. and Abdel-Hafez, M.F., "Intelligent attitude and flapping angles estimation of flybarless helicopters under near-hover conditions," *Journal of the Franklin Institute*, Vol.355, No.14, pp.6830-6858 (2018).

Bian, H.W., Jin, Z.H. and Tian, W.F., "IAE-adaptive Kalman filter for INS/GPS integrated navigation system," *Journal of Systems Engineering and Electronics*, Vol.17, No.3, pp.502-508 (2006).

El-Rabbany, A., *Introduction to GPS: The Global Positioning System*, Artech (2011).

Fang, J.C. and Yang, S., "Study on Innovation Adaptive EKF for In-Flight Alignment of Airborne POS," *IEEE Transactions on Instrumentation and Measurement*, Vol.60, No.4, pp.1378-1388 (2011).

Feng, K.Q., Li, J., Zhang, D.B., Wei X.K. and Yin, J.P., "Robust Cubature Kalman Filter for SINS/GPS Integrated Navigation Systems with Unknown Noise Statistics," *IEEE Access*, Vol.9, pp. 9101-9116 (2021).

Huang, D.L., Henry, L. and El-Sheimy, N., "Expectation maximization based GPS/INS integration for land vehicle navigation," *IEEE Transactions on Aerospace and Electronic Systems*, Vol.43, No.3, pp.1168–1177 (2007).

Huang, Y.L., Zhang, Y.G., Li, N., Wu, Z.M. and Chambers J.A., "A Novel Robust Student's-Based Kalman Filter," *IEEE Transactions on Aerospace and Electronic Systems*, Vol.53, No.3, pp.1545-1554 (2017).

Huang, Y.L., Zhang, Y.G., Xu, B., Wu, Z.M. and Chambers J.A., "A New Adaptive Extended Kalman Filter for Cooperative Localization," *IEEE transactions on aerospace and electronic systems*, Vol.54, No.2, pp. 353-368 (2018).

Karlgaard, C.D. and Schaub, H., "Huber-based divided difference filtering," *Journal of Guidance, Control and Dynamics*, Vol.30, No.3, pp. 885–891 (2007).

Lai, X., Zhu, G.R. and Chambers, J.A., "A fuzzy adaptive extended Kalman filter exploiting the Student's t distribution for mobile robot tracking," *Measurement Science and Technology*, Vol.32, No.10, pp. 105017 (2021).

Li, D.G., Wu, Y.Q. and Zhao, J.M., "Novel Hybrid Algorithm of Improved CKF and GRU for GPS/INS," *IEEE Access*, Vol.8, pp.202836-202847 (2020).

Li, K.L., Hu, B.Q., Chang, L.B. and Li, Y., "Comparison of direct navigation mode and indirect navigation mode for integrated SINS/GPS," *Transactions of the Institute of Measurement and Control*, Vol.38, No.1(2016), pp.3-13 (2016).

Li, P., Li, C., Wu, X.J. and Chen, Z.G., "A Modified IAE Algorithm for GNSS and IMU Integration," *Lecture Notes in Electrical Engineering*, Vol.187, pp.427-437 (2013).

Li, W., Liu, M.H., Gong, D.R and Duan, D.P., "Huber-based divided difference filter with application to relative navigation," *Proceedings of the Institution of Mechanical Engineers*, Vol.228, No.9, pp. 1475-1486 (2014-1).

Li, W., Liu, M. H. and Duan, D., "Adaptive Huber-based Kalman filtering for spacecraft attitude estimation," *Transactions of the Institute of Measurement and Control*, Vol.36, No.6, pp.828-836 (2014-2).

Li, Y., Gao, S.S. and Yang, Y., "A Novel Adaptive UKF and its Application in the SINS/GPS Integrated Navigation," *Applied Mechanics and Materials*, Vol.3337, No.1194, pp.521-524 (2014).

Liu, J.J., Chen, H.M. and Liu, N.B., "Effective Sage-Husa Kalman filter for SINS/Doppler/Platform

Compass integrated navigation system," Proceedings of 2016 IEEE Navigation and Control Conference, Nanjing, China, pp.542-547 (2016).

Mohamed, A.H. and Schwarz, K.P., "Adaptive Kalman Filtering for INS/GPS," *Journal of Geodesy*, Vol.73, No.4, pp. 193-203 (1999).

Narasimhappa, M., Mahindrakar, A.D., Guizilini, V.C., Terra, M.H. and Sabat, S.L., "MEMS-Based IMU Drift Minimization: Sage Husa Adaptive Robust Kalman Filtering," *IEEE Sensors Journal*, Vol.20, No.1, pp.250-260 (2020).

Narasimhappa, M., Rangababu, P., Sabat, S.L. and Nayak, J., "A modified Sage-Husa adaptive Kalman filter for denoising Fiber Optic Gyroscope signal," Proceedings of 2012 Annual IEEE India Conference, Kochi, India, pp.1266-1271 (2012).

Ning, X.L., Yuan, W.P. and Liu, Y.H., "A tightly coupled rotational SINS/CNS integrated navigation method for aircraft," *Journal of systems engineering and electronics*, Vol.30, No. 4, pp.770-782 (2019).

Qian, H.M., An, D. and Xia, Q.X., "IMM-UKF based land-vehicle navigation with low-cost GPS/INS," Proceedings of 2010 IEEE International Conf. on Information and Automation, Haerbin, China, pp. 2031-2035 (2010).

Ren, J.X., Zi, J.L., Yang, H. and Li, J., "Performance Analysis and Architectures for a MEMS-SINS/GPS Ultratight Integration System," *Mathematical Problems in Engineering*, Vol.2021, No.1, pp. 1-13 (2021).

Sage, A. and Husa, G., "Algorithms for sequential adaptive estimation of prior statistics," *Proceedings of the 8th IEEE Symposium on Adaptive Processes Decision and Control*, pp. 61 (1969).

Schön, T.B., Wills, A. and Ninness, B., "System identification of nonlinear state-space models," *Automatica*, Vol.47, No.1, pp. 39-49 (2022).

Tripathi, R.P., Singh, A.K. and Gangwar, P., "Innovation-based fractional order adaptive Kalman filter," *Journal of Electrical Engineering*, Vol.71, No.1, pp. 60-64 (2020).

Tseng, C.H., Lin, S.F, and Jwo, D.J., "Robust Huber-Based Cubature Kalman Filter for GPS Navigation Processing", *Journal of Navigation*, Vol.70, No.3, pp. 527-546 (2017).

Wang, J., Liu, J. and Cai, B.G., "Study on Information Fusion Algorithm in Embedded Integrated Navigation System," Proceedings of IEEE 2008 International Conference on Intelligent Computation Technology and Automation, Changsha, China, pp. 1007–1010 (2008).

Wang, L., Cheng, X., Liu, C., Li, J. and Duan, Y., "Huber-based rank Kalman filtering algorithm for mobile robot in complex environment," *Zhongguo Guanxing Jishu Xuebao*, Vol.27, No.1, pp. 60-65 (2019).

Wang, Y.C. and Li, Y., "The positioning principle of global positioning system and its application prospects," *IOP Conference Series: Earth and Environmental Science*, Vol.781, No.2, pp. 022085 (2021).

Wang, Z., An, H. and Luo, X.L., "Adaptive filtering-based recursive identification for time-varying Wiener output-error systems with unknown noise statistics," *Journal of the Franklin Institute*, Vol.357, No.2, pp.1280-1298 (2020).

Xu, S.Q., Zhou, H.Y., Wang, J.Q., He, Z.M. and Wang, D.Y., "SINS/CNS/GNSS Integrated Navigation Based on an Improved Federated Sage-Husa Adaptive Filter," *Sensors*, Vol.19, No.17, pp. 3812 (2019).

基於未知雜訊的SINS/GPS 組合導航新穎魯棒卡爾曼濾波演算法

賴欣 楊福鑫

西南石油大學機電工程學院

石油天然氣裝備技術四川省科技資源分享服務平臺

油氣藏地質及開發工程國家重點實驗室

摘 要

在實際應用中，由於環境雜訊和載體運動時的機動等因素的影響，過程雜訊的估計往往不準確。因此提高組合導航系統的精度和穩定性對車輛和飛機等系統至關重要。針對組合導航系統中未知參數估計的不確定性問題，提出了一種魯棒的基於期望最大化的卡爾曼濾波(EM-KF)演算法。採用線上期望最大化(EM)方法自我調整估計預測誤差協方差矩陣和測量雜訊協方差矩陣。本文提出的EM-KF演算法的顯著優點包括：該演算法利用線上 EM 演算法對參數進行最大似然估計，每次反覆運算的最大似然估計隨著似然增量的增加而收斂，保證了反覆運算的局部收斂性；自我調整估計預測誤差協方差矩陣和測量雜訊協方差矩陣可以減少對先驗資訊的依賴並減少雜訊對測量估計的影響；本文所提出的 EM-KF 在複雜環境下具有良好的導航精度和魯棒性。模擬和現場測試結果表明，該演算法具有較強的魯棒性和精度，能夠實現長時間的高精度移

動車輛導航。